Spin-parity analysis of diffractive $np \to (p\pi^-)p$ and the question of a parity-change rule

J. G. Rushbrooke, R. Raja, R. E. Ansorge, J. R. Carter, and W. W. Neale
*Cavendish Laboratory, Cambridge, England**
(Received 7 October 1975)

A spin-parity analysis is performed of the low-mass (≤ 1.75 GeV/c^2) $p\pi^-$ system in diffractive $np \to (p\pi^-)p$ using new data at 13 GeV/c and 20 GeV/c. In the context of a Deck-plus-resonances model a good fit to the $p\pi^-$ angular moments is found only if the Gribov-Morrison parity-change rule does not hold and spin states up to $j = \frac{5}{2}$ are included. In particular the presence of a considerable fraction of spin-parity $\frac{1}{2}^-$ state is indicated.

I. INTRODUCTION

The process of diffraction dissociation (DD) of hadrons has been clearly identified experimentally,[1] but still awaits a satisfactory theoretical explanation. An important question for any theory of DD is whether or not there exists a parity-change rule, such as that proposed by Morrison,[2] which has come to be known as the Gribov-Morrison rule.[3] To establish such a rule experimentally will obviously require measurements of the spin-parity composition of dissociated systems, knowledge of which will further our understanding of DD whether or not a parity-change rule exists.

Spin-parity analyses of meson dissociations have been carried out in some detail for 3π[4] and $K\pi\pi$[5] systems. These tend to show that the DD cross section is to a large extent made up of final states (A_1, Q, ...) obeying the proposed Gribov-Morrison (GM) rule $\Delta P = (-1)^{\Delta J}$, for the change in parity ΔP and spin ΔJ between the initial particle and the dissociated system. However, an important exception to this rule is possibly the A_2 meson which has recently been observed[6] in coherent production off nuclei. It is probably fair to say, therefore, that the GM rule lacks firm experimental and theoretical support here.

Nucleon DD is even less well understood. In the 3-body reactions $\pi N \to \pi(N\pi)$ and $NN \to N(N\pi)$ a broad low-mass $(N\pi)$ enhancement has been identified as DD using the technique of isospin analysis to isolate isoscalar exchange. Complete spin-parity analyses of these reactions, which would require measurements of nucleon polarizations, have not been attempted. There have been some analyses[7] of $I = \frac{1}{2}$ $N\pi$-system decay distributions, but these analyses *assume* that only the P_{11}, D_{13}, and F_{15} partial waves (i.e. $\frac{1}{2}^+$, $\frac{3}{2}^-$, and $\frac{5}{2}^+$ final states) contribute in accordance with the GM rule, rather than trying to test the rule itself. A more recent study[8] of $\pi N \to \pi(N\pi)$ at 14 GeV/c has used the reaction $\pi N \to \pi\Delta$ as a partial-wave analyzer for DD, and has shown that a considerable fraction of the diffractive πN system in the Δ mass region (< 1.325 GeV/c^2) is comprised of the S_{11} wave (i.e., $\frac{1}{2}^-$ final state), in disagreement with the rule.

Without nucleon polarization measurements a spin-parity analysis of nucleon DD can only be made within the framework of a particular model. In this paper we present an analysis of new data on $np \to (p\pi^-)p$ in the momentum range 9–24 GeV/c, using a model which combines a one-pion-exchange (i.e., Deck) amplitude and a diffractive $N^*_{1/2}$ resonance production amplitude. We show that this model is able to give a satisfactory explanation of $p\pi^-$ mass distributions and decay angular moment distributions. To calculate angular moments means evaluating interferences between the amplitudes for Deck and resonance production in different partial waves, and hence knowledge of the partial-wave composition of the Deck amplitude is required. The Deck model affords a natural explanation of the bump in the $N\pi$ mass distribution below 1.40 GeV observed in all the above experiments; this avoids assuming[9] *a priori* some quasiresonant $N^*(1300)$ state produced in DD, at a lower mass than and distinct from the $\pi N \to \pi N$ partial-wave-analysis resonances (though these explanations are possibly related in the sense of duality). Interpretations of the A_1 enhancement in terms of a Deck model have already met with success.[4]

In Sec. II the spin-parity formalism for a moments analysis is described, the underlying assumptions (such as t-channel helicity conservation, etc.) discussed in relation to the experimental data, and formulas are given for the angular moments. In Sec. III details of the partial-wave decomposition of the Deck amplitude are given and the model used in the spin-parity analysis is described. The procedure for fitting the model to the experimental data, and the results of the fit, are given in Sec. IV.

II. SPIN-PARITY FORMALISM FOR $N \to N\pi$

A. Formula

We are seeking information on the spin and parity of the $N\pi$ system produced diffractively according to Fig. 1(a), where A is an unspecified hadron. One assumes, in accordance with observation,[10] that the DD amplitude is factorizable in the t channel. The t-channel exchange may be characterized by a naturality quantum number ϵ; at high energy one expects $\epsilon = +1$ (natural-parity exchange) to dominate,[11] e.g., the Pomeron pole. We assume further that t-channel helicity conservation (TCHC) holds, or is at least dominant; the experimental situation here will be discussed below. Then there is only one independent amplitude for each spin j and parity η of the $N\pi$ system, which we label as L_{2j}, where L is the spectroscopic symbol for the angular momentum $l = j \pm \frac{1}{2}$, with $\eta = -(-1)^l$. Each amplitude is a function of s, t, and the $N\pi$ mass m.

The spin-parity information is to be obtained from measurements of the moments $\langle \sigma Y_{JM} \rangle$ of the decay angular distribution $W(\theta, \phi)$, defined by

$$\langle \sigma Y_{JM} \rangle = \int W(\theta, \phi)\, Y_{JM}(\theta, \phi)\, d\Omega \,. \tag{2.1}$$

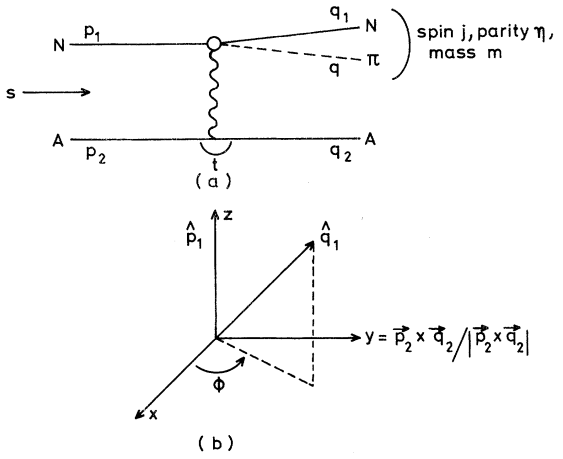

FIG. 1. (a) Diagram for diffractive process $NA \to (N\pi)A$ where A is a hadron. (b) Decay angles (θ, ϕ) of nucleon in the Gottfried-Jackson frame.

The angles (θ, ϕ) may be taken as those of the decay nucleon in the Gottfried-Jackson[12] or t-channel helicity frame, with the z axis along the incident nucleon direction and the y axis normal to the production plane [see Fig. 1(b)]. With the above assumptions it can be shown[13] that

$$\langle \sigma Y_{JM} \rangle = \tfrac{1}{2} \sum_{j,j',l,l'} \left[\frac{(2j+1)(2j'+1)}{4\pi(2J+1)} \right]^{1/2} [1 + (-1)^{J+l+l'}] \langle jj' - \tfrac{1}{2}\tfrac{1}{2} | JO \rangle^2 \delta_{MO} \delta_{\epsilon\epsilon'} L_{2j} L^*_{2j'} \,. \tag{2.2}$$

Moments that can be nonvanishing are those with $J \leq j + j'$. The important result that only $M = O$ moments are nonvanishing is a consequence of TCHC, which has the absence of ϕ dependence as a necessary condition. Also, without TCHC there would be an unmanageable number of amplitudes: $(2j+1)$ for each j^η, in fact. In writing (2.2) we have allowed the naturality ϵ to be different for production of different j^η's (amplitudes of the same j^η and different ϵ's do not interfere). This is because in practice the $\frac{3}{2}^+$ state often contains a significant Δ contribution, for which one expects a strong π-exchange (unnatural-parity) contribution. So we shall assume there is a P_3^- amplitude with $\epsilon = -1$, but that all other amplitudes have $\epsilon = +1$, which we write S_1, P_1, P_3, D_3, ...

If $\langle \sigma Y_{JO} \rangle \neq 0$ for, say, $J \leq 5$ only, this means we need only include $j \leq \frac{5}{2}$ amplitudes. Formulas for these moments are then as follows:

$$\sqrt{4\pi}\, \langle \sigma Y_{00} \rangle = |S_1|^2 + |P_1|^2 + |P_3|^2 + |P_3^-|^2 + |D_3|^2 + |F_5|^2 \,, \tag{2.3}$$

$$\sqrt{12\pi} \langle \sigma Y_{10} \rangle = 2\,\mathrm{Re}(S_1^* P_1) + 2\sqrt{2}\,\mathrm{Re}(S_1^* P_3) + 2\sqrt{2}\,\mathrm{Re}(P_1^* D_3) + \tfrac{2}{5}\mathrm{Re}(P_3^* D_3) + \frac{6\sqrt{6}}{5}\mathrm{Re}(P_3^* D_5) + \frac{6\sqrt{6}}{5}\mathrm{Re}(D_3^* F_5) + \tfrac{6}{35}\mathrm{Re}(D_5^* F_5) \,, \tag{2.4}$$

$$\sqrt{20\pi}\, \langle \sigma Y_{20} \rangle = 2\sqrt{2}\,\mathrm{Re}(S_1^* D_3) + 2\sqrt{3}\,\mathrm{Re}(S_1^* D_5) + 2\sqrt{2}\,\mathrm{Re}(P_1^* P_3) + 2\sqrt{3}\,\mathrm{Re}(P_1^* F_5) + |P_3|^2 + \frac{2\sqrt{6}}{7}\mathrm{Re}(P_3^* F_5) + |D_3|^2 + \frac{2\sqrt{6}}{7}\mathrm{Re}(D_3^* D_5) + \tfrac{8}{7}|D_5|^2 + \tfrac{8}{7}|F_5|^2 + |P_3^-|^2 \,, \tag{2.5}$$

$$\sqrt{28\pi}\, \langle \sigma Y_{30} \rangle = 2\sqrt{3}\,\mathrm{Re}(S_1^* F_5) + 2\sqrt{3}\,\mathrm{Re}(P_1^* D_5) + \tfrac{18}{5}\mathrm{Re}(P_3^* D_3) + \frac{4\sqrt{6}}{5}\mathrm{Re}(P_3^* D_5) + \frac{4\sqrt{6}}{5}\mathrm{Re}(D_3^* F_5) + \tfrac{16}{15}\mathrm{Re}(D_5^* F_5) \,, \tag{2.6}$$

$$\sqrt{36\pi}\, \langle \sigma Y_{40} \rangle = \frac{12\sqrt{6}}{7}\mathrm{Re}(P_3^* F_5) + \frac{12\sqrt{6}}{7}\mathrm{Re}(D_3^* D_5) + \tfrac{6}{7}|D_5|^2 + \tfrac{6}{7}|F_5|^2 \,, \tag{2.7}$$

$$\sqrt{44\pi}\, \langle \sigma Y_{50} \rangle = \tfrac{12}{7}\mathrm{Re}(D_5^* F_5) \,. \tag{2.8}$$

As mentioned above there are no terms involving interference between the natural-parity-exchange amplitude and P_3^-; the term $|P_3^-|^2$ appears in σ and $\langle \sigma Y_{20} \rangle$ only, and its presence can be simply subtracted out, as we shall see in the next section.

B. Selection of data

We now turn to a more detailed consideration of the assumptions underlying Eq. (2.2) in relation to experiment. We present new data on the reaction $np \to pp\pi^-$ at 9–24 GeV/c, based on 5966 events obtained from an exposure of the CERN 2-m hydrogen bubble chamber to a neutron beam; basic details of this experiment have been described elsewhere.[14] The final protons are labeled p_f and p_s according to their c.m.s. production cosines ($\cos\theta_f^* > \cos\theta_s^*$). The quantity $t' = |t - t_{\min}|$ between p_s and the target proton is shown in Fig. 2(a), and Figs. 2(c) and 2(d) give distributions in $m(p_f\pi^-)$ and $m(p_s\pi^-)$. The c.m.s. production cosine of the π^- [Fig. 2(b)] is found to have a minimum at about -0.3 which may be used to associate the pion with either p_f or p_s, following a method established by Dahl-Jensen *et al.*[15] We define two event samples,

(a) $np \to (p_f\pi^-)p_s$ ($\cos\theta_\pi^* > -0.3$, 5178 events),

(b) $np \to p_f(p_s\pi^-)$ ($\cos\theta_\pi^* < -0.3$, 788 events),

which are shown as the dashed histograms in Figs. 2(c) and 2(d). The former shows a large diffractive bump centered on about 1.35 GeV/c^2 and the latter shows a strong Δ^0 signal. The analysis will be based on sample (a), which we represent by the diagram shown in Fig. 3(a).

We can infer from a recent isospin analysis[15] of $NN \to N(N\pi)$ that 90–95% of the cross section for Fig. 3(a) proceeds by t-channel isospin $I_t = 0$ exchange in the momentum range covered by this experiment. Furthermore, a substantial part of the remaining 5–10% is the production of $p_f\pi^-$ in an $I = \frac{3}{2}$ state, necessarily by $I_t = 1$ exchange. One can show from isospin that there should be equal amounts of Δ^0 production in both the above event samples (a) and (b). We see a clear $\Delta^0(p_s\pi^-)$ signal of approximately 200 events in the dashed histogram of Fig. 2(d); we therefore know that

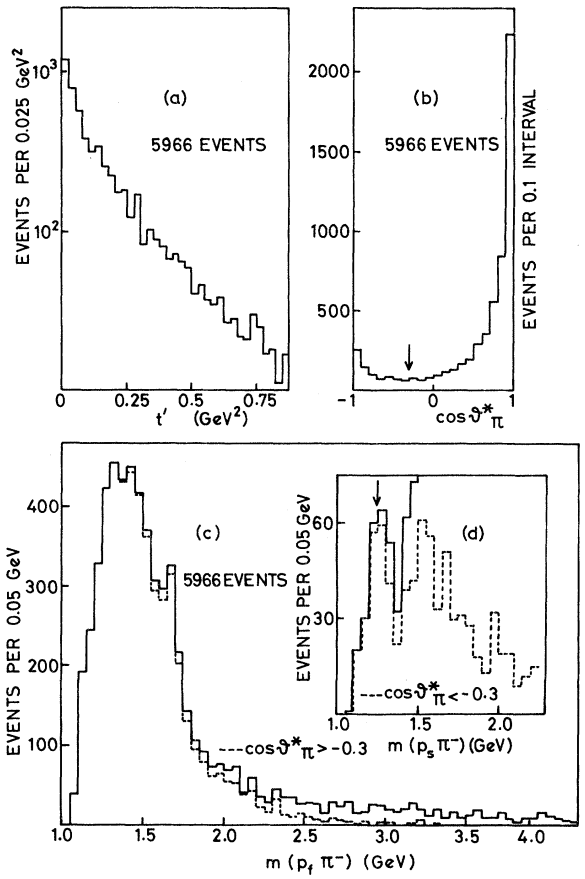

FIG. 2. Experimental distributions for events $np \to pp\pi^-$ at 9–24 GeV/c, where the final protons are labeled p_f and p_s according to their c.m.s. production cosines. (a) $t' = |t - t_{\min}|$ between p_s and target proton; (b) c.m.s. cosine of pion; (c) distributions in $m(p_f\pi^-)$, and (d) in $m(p_f\pi^-)$. The dashed histograms in (c) and (d) are obtained after associating the pion with either proton as indicated.

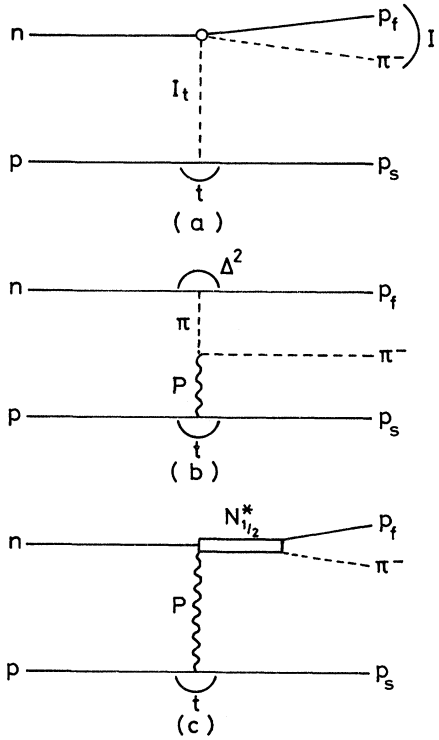

FIG. 3. Diagrams for $np \to (p_f\pi^-)p_s$ as defined in the text.

there is about 200/5178 = 4% of $\Delta^0(p_f\pi^-)$ included in sample (a). We take the unnatural-parity-exchange amplitude P_3^- to represent $\Delta^0(p_f\pi^-)$ production by π exchange, since the analysis of Dahl-Jensen *et al.*[15] has shown that production of the $I=\frac{3}{2}$ $N\pi$ state in $NN \to N(N\pi)$ is mainly by π exchange. The effect of this $\Delta^0(p_f\pi^-)$, via $|P_3^-|^2$ only in (2.3) and (2.5) for $\langle \sigma Y_{00}\rangle$ and $\langle \sigma Y_{20}\rangle$, respectively, can be subtracted out. This was done by subtracting from the value of N_i (the number of events) and $\langle N_i Y_{20}\rangle$ in each ith bin of $m(p_f\pi^-) < 1.3$ GeV, the corresponding values for $p_s\pi^-$ (involving about 145 events after the t' cuts described below). We therefore conclude that our sample of $np \to (p_f\pi^-)p_s$ events to be analyzed is $\gtrsim 95\%$ $I_t = 0$ exchange; the remaining $\lesssim 5\%$ will be mostly $I = \frac{1}{2}$ $N\pi$ produced by $I_t = 1$ exchange.

For convenience these events of type (a) were subdivided into two data sets having neutron beam momentum p_0 above and below 16 GeV/c, and the further restrictions $t' < 0.2$ GeV^2 and $m(p_f\pi^-) < 1.75$ GeV/c^2 were made for this analysis. Experimental distributions in the number of events N and the angular moments $\langle Y_{J0}(\theta, \phi)\rangle$ in each bin of $m(p_f\pi^-)$ were determined for the data sets

(A) $9 < p_0 < 16$ GeV/c ($\langle p_0\rangle = 12.7$ GeV/c, 1290 events),

(B) $16 < p_0 < 24$ GeV/c ($\langle p_0\rangle = 19.9$ GeV/c, 1807 events),

and are shown in Fig. 4 for J up to 3. As a check on any t' dependence we shall also refer to a third data set for which $t' < 0.1$ GeV^2 and $m(p_f\pi^-) < 1.75$ GeV/c^2, but with no p_0 selection (since there is little p_0 dependence in our data) to get adequate statistics:

(C) $9 < p_0 < 24$ GeV/c ($\langle p_0\rangle = 16.6$ GeV/c, 2323 events).

In addition to Fig. 4 the moments $\langle \mathrm{Re}Y_{LM}\rangle$ and $\langle \mathrm{Im}Y_{LM}\rangle$ for $M \neq 0$ were consistent with zero except for $\langle \mathrm{Re}Y_{11}\rangle$ and to a lesser extent $\langle \mathrm{Re}Y_{21}\rangle$; some of these are shown in Fig. 5. We recall that to avoid an unmanageable number of amplitudes our analysis requires TCHC, which means that these real moments should vanish, so the implications of this result for our analysis will now be discussed.

C. t-channel helicity conservation

Our event sample shows clear evidence of TCHC violation; similar effects have been seen in other experiments[16] at about the same level. We shall now demonstrate that this effect does not invalidate our analysis, or may only do so at a level below a few percent.

The fact that $\langle \mathrm{Re}Y_{11}\rangle$ and $\langle \mathrm{Re}Y_{21}\rangle$ are nonzero implies a $\cos\phi$ dependence which is apparent in Fig. 6 for data set (C); the ϕ distribution is of the form $W(\phi) \propto 1 - 0.29\cos\phi$. Now any ϕ dependence enters the diffractive amplitude in the form $e^{i(\lambda_n - \lambda)\phi}$, where λ_n is the helicity of the incoming neutron and λ is the z component of j (in the t-channel frame defined above). We therefore write the amplitude in the form $A = \alpha + \beta e^{i\phi}$, where α and β are TCHC-obeying and TCHC-violating parts, respectively, (independent of ϕ). On requiring no $\sin\phi$ dependence so that $\langle \mathrm{Im}Y_{J1}\rangle = 0$, as observed (and as required by parity conservation), we have

$$W(\phi) \propto |A|^2 = |\alpha|^2 + |\beta|^2 \pm 2|\alpha||\beta|\cos\phi\,,$$

from which the data give $|\alpha|^2 = 0.98$, $|\beta|^2 = 0.022$. Equation (2.1) then means that

$$\langle \sigma Y_{J0}\rangle \propto \int (|\alpha|^2 + |\beta|^2)\, Y_{J0}\, d\Omega\,,$$

and so the values of $\langle \sigma Y_{J0}\rangle$ which we shall use in our analysis are affected by the TCHC-violating part only at the 2% level. This justifies our inclusion of only TCHC-satisfying amplitudes in the model analysis to be described.

The same analysis was carried out in each bin of $m(p_f\pi^-)$, and the above effect was always below 3%: the result was similar with data sets A and B.

Finally, we observe that larger amounts of helicity flip (such as $e^{2i\phi}$ in the amplitude) are absent since the moments for $M \geq 2$ are consistent with zero.

Before leaving the subject of a ϕ dependence of the data, we refer to the dashed histogram of Fig. 6. This subset of the data was obtained after further requiring backward Jackson angles, $\cos\theta < -0.5$, and shows no ϕ dependence. According to the recent arguments of Berger,[17] this is to be interpreted as revealing that there is no nucleon exchange occurring, and that these events probably arise from resonance production. The ϕ-dependent events at forward Jackson angles can come (according to Berger) from pion exchange. The above arguments apply equally to events in any region of $m(p_f\pi^-)$, and substantiate the pion-exchange-plus-resonance model employed in this analysis.

D. Summary

The above formulas (2.3) to (2.8) for the moments $\langle \sigma Y_{J0}\rangle$ depend on a diffractive amplitude with the following properties:

a. factorizability in the t channel,

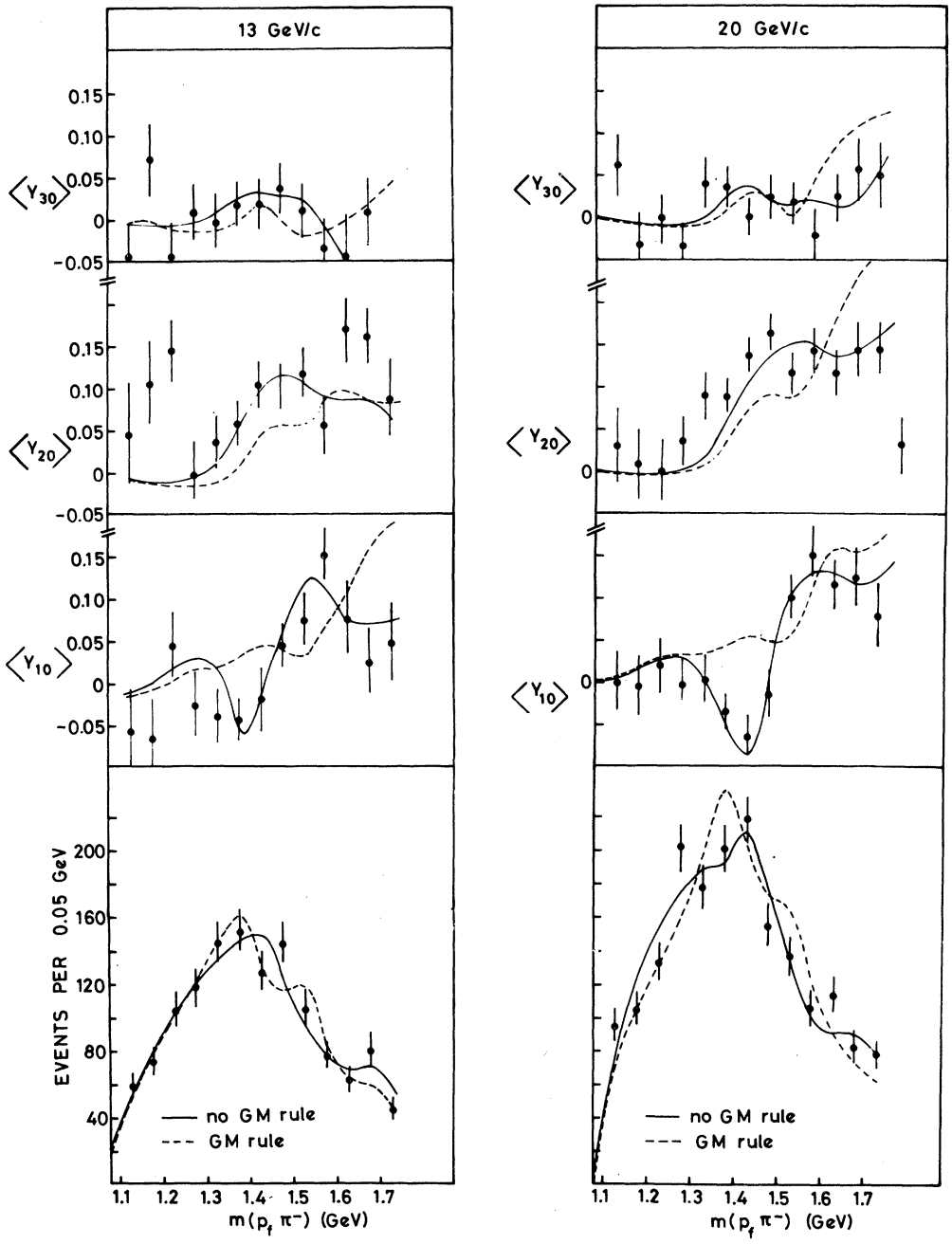

FIG. 4. Mass and angular moment distributions for $np \to (p_f \pi^-)p_s$ at 13 and 20 GeV/c, for $t' < 0.2$ GeV^2 (data sets A and B). The full curves are the fits obtained with the model described in Sec. IV, without the Gribov-Morrison rule. The dashed curves are from the best fit that could be obtained assuming the rule to be true (see text).

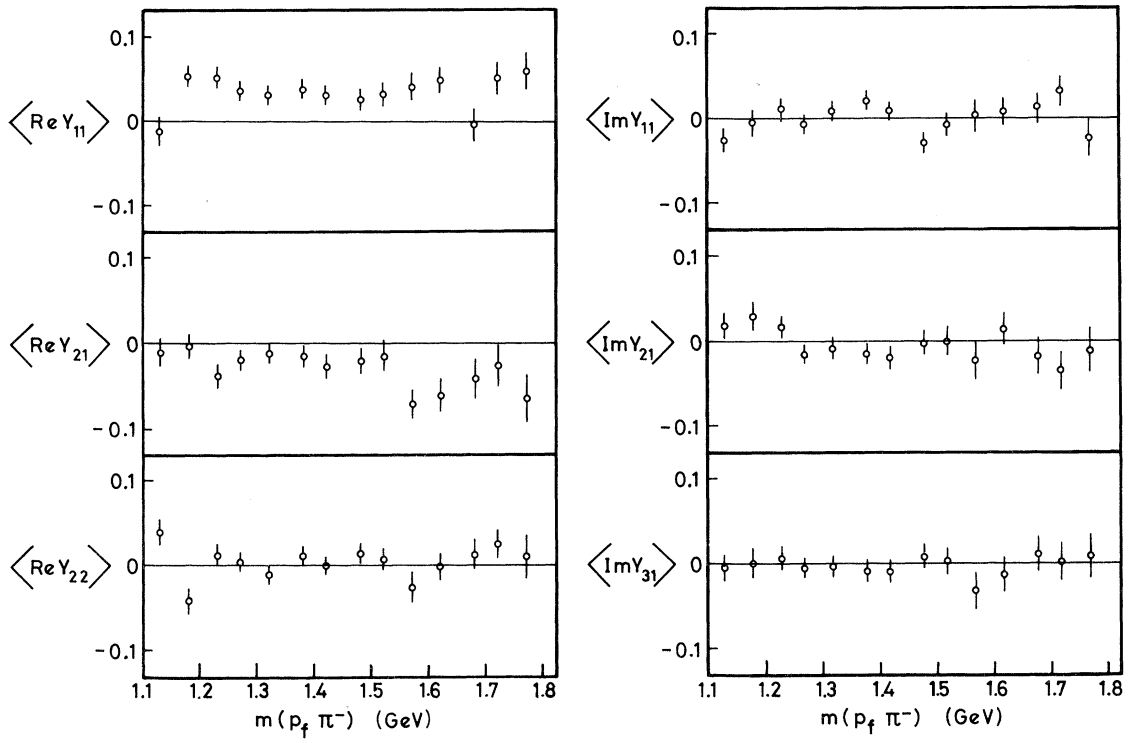

FIG. 5. Angular moment distributions for $np \to (p_f \pi^-)p_s$ for $t' < 0.1$ GeV^2, and $9 < p_0 < 24$ GeV/c (data set C).

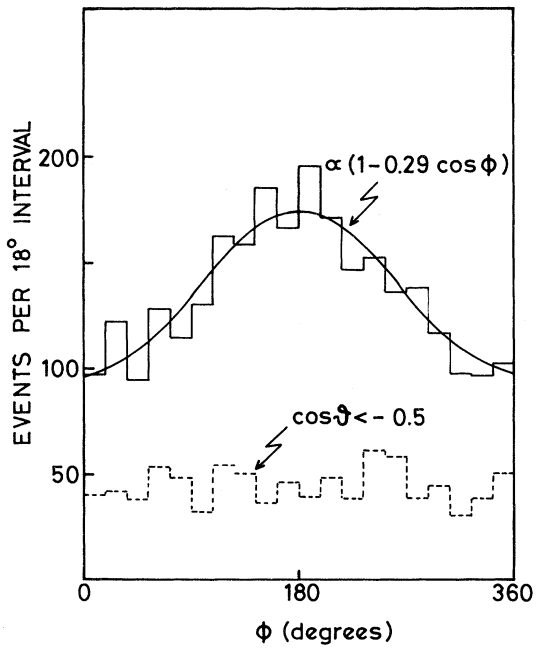

FIG. 6. Distribution in ϕ for $np \to (p_f \pi^-)p_s$ for $t' < 0.1$ GeV^2 and $9 < p_0 < 24$ GeV/c (data set C). The dashed histogram is for the further restriction to events having $\cos\theta < -0.5$.

b. natural-parity exchange, which is assumed to be in the Pomeron P,

c. TCHC,

d. $j \lesssim \frac{5}{2}$ only (since $\langle Y_{J0} \rangle$ is consistent with zero for $J \geq 6$).

In view of the discussion of the previous sections we shall assume that our data sample is consistent with these assumptions.

III. DECK-PLUS-RESONANCE MODEL

A. Introduction

As indicated in Sec. I, we choose as model amplitude a sum of one-pion exchange [i.e., the Deck diagram, Fig. 3(b)] and resonance production [Fig. 3(c)]. According to duality the latter would be equivalent to A_2 and other (non-π) exchange in a double-Regge-exchange model. The exchange at the bottom vertex in Fig. 3(b) is assumed to be dominated by the Pomeron; our data show a small ($\lesssim 5\%$) $I_t = 1$ exchange (see Sec. II B), and this would be naturally represented by a small amount of ρ (and other non-Pomeron) exchange included in the diffractive vertex of Fig. 3(b).

We exclude from consideration other model dia-

grams such as nucleon exchange for the reasons given in Sec. II C. We also neglect absorptive corrections to the Deck amplitude, which have been shown[18] not to affect the major features of the low-mass enhancement, such as spin-parity content and mass and angular distributions, at low $|t|$ ($\lesssim 0.3$ GeV^2).

To calculate the interferences between the diagrams of Figs. 3(b) and 3(c) one requires knowledge of the partial-wave composition of the Deck amplitude, which will now be discussed.

B. Deck amplitude in partial waves

The partial-wave analysis of the deck amplitude for $NN \to N(N\pi)$ has been considered by Resnick[19] and by Rushbrooke.[20] It can be shown that the partial cross section for producing a $p_f\pi^-$ state of spin j, parity η, and mass m, according to the diagram of Fig. 3(b), is given by the expression

$$\frac{d^2\sigma}{dm\,dt} = (2\pi)^{-5}\frac{f_I g(t)}{2^8 M^2 p_L^2} q\left(j+\frac{1}{2}\right)|U|^2 , \tag{3.1}$$

with

$$\eta = (-1)^{j\pm 1/2}: U = i4\pi\sqrt{2}G\int_{-1}^{1} dz[J_+J'_- P_{j\pm 1/2}(z) - J_-J'_+ P_{j\pm 1/2}(z)](\Delta^2+\mu^2)^{-1}h(z)F(\Delta^2) , \tag{3.2}$$

where $J_\pm = (E_n \pm M)^{1/2}$, $J'_\pm = (E_f \pm M)^{1/2}$, $z = -\cos\theta$. The factor f_I allows for isospin and is equal to 2; μ is the pion mass, M is the nucleon mass, and the coupling strength G is given by $G^2/4\pi = 14.4$; p_L is the laboratory momentum of the beam neutron; E_n and E_f are the total energies of the neutron and p_f in the rest frame of $p_f\pi^-$, and q is the three-momentum of the π^- in that frame. Δ^2 is the four-momentum squared of the exchanged pion, which is assumed to scatter diffractively from the target proton (making U pure imaginary). At this $\pi N \to \pi N$ vertex the t dependence is given by $g(t) = \exp(bt + ct^2)$; values $b = 9$, $c = 2.5$ from experimental data were taken ($\Delta^2 > 0$ and $t < 0$ in the physical region). $F(\Delta^2)$ is a form factor to be determined by comparison with the data. The function $h(z)$ is defined as

$$h(z) = \frac{1}{4\pi}\int_0^{2\pi} (\omega^2 - M^2)\sigma_{\text{tot}}(\omega)d\phi , \tag{3.3}$$

where $\sigma_{\text{tot}}(\omega)$ is the total cross section of πN scattering and ω is the invariant energy. [The manner of calculation of $h(z)$ is indicated in Refs. 19 and 20, though there the asymptotic approximation $\sigma_{\text{tot}} \approx 28$ mb was used and this factor was not included in the definition of $h(z)$.] The integrand is of course a function of ϕ, which means that the Deck amplitude has a TCHC-violating component (as implied in Sec. II C). One can show by direct calculation that the influence of this part of the amplitude on model values of $\langle Y_{J0}\rangle$ is $< 10\%$, and will not significantly disturb our solutions for TCHC-satisfying amplitudes. The ϕ dependence of the Deck model is qualitatively in accord with that of our data (such as is shown in Fig. 6), but any quantitative investigation of the $M \neq 0$ moments would lie outside the scope of this analysis for the reasons given in Sec. II.

At this point we recall that the Deck amplitude alone is to explain the characteristic enhancement at about 1.35 GeV/c^2 in the mass spectrum (Figs. 4 and 7), which is well below the mass of known nucleon resonances. We have chosen a function $F(\Delta^2)$ which brings the Deck model into agreement with the experiment for masses $\lesssim 1.35$ GeV^2. Provided one ensures a fairly sharp cut-off with Δ^2 the exact choice of function is not critical in that the relative contribution of different partial waves are essentially unaffected; we have used a Gaussian $F(\Delta^2) = \exp[-2(\Delta^2+\mu^2)^2]$, and the result is shown in Fig. 8. The curves drawn are the values of $\int(d^2\sigma/dm\,dt)dt$, where the integral runs over $0 < t' < 0.1$ GeV^2, for each partial wave separately, and for the sum over all partial waves.

There is a further calculational point; in confronting the data we need partial-wave cross sections integrated over t, whereas the formulas (2.3)–(2.8) are in terms of amplitudes (with appropriate phases). We adopt the expedient of taking the Deck amplitude in any partial wave k (standing for spin j and parity η) to be

$$D_k \equiv i\eta(-1)^{j-1/2}\left\{\int\frac{d^2\sigma}{dm\,dt}\,dt\right\}^{1/2} , \tag{3.4}$$

where we have preserved the phase of U in the manner indicated (the sign of U in a given partial wave may be shown to be the same at all values of u and t). Values of $\langle Y_{J0}\rangle$ calculated from (3.4) for the range $t' < 0.1$ GeV^2, according to Eqs. (2.4)–(2.6), are shown for $J = 1$, 2, 3 as the dot-dashed curves in Fig. 7. There is seen to be considerable disagreement with the data points [set (C)]. Equi-

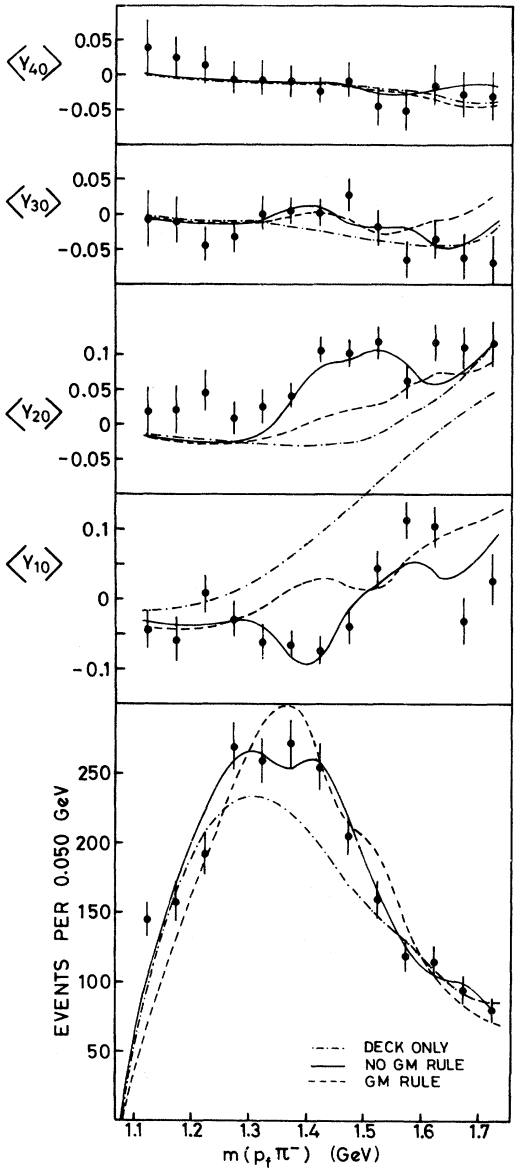

FIG. 7. Mass and angular moment distributions for $np \to (p_f\pi^-)p_s$ for $t' < 0.1$ GeV^2, and $9 < p_0 < 24$ GeV/c (data set C). The solid curves are the fits obtained with the model described in Sec. IV, without the Gribov-Morrison rule. The dashed curves are from the best fit that could be obtained assuming the rule to be true (see text). The dot-dashed curves are the predictions of the Deck model alone.

valently, we show $m(p_f\pi^-)$ distributions for the Jackson angle selections (a) $\cos\theta > 0$ and (b) $\cos\theta < 0$ as the dot-dashed curves in Fig. 9 where again there is marked disagreement with the data. We now try to resolve these disagreements by the inclusion of resonances.

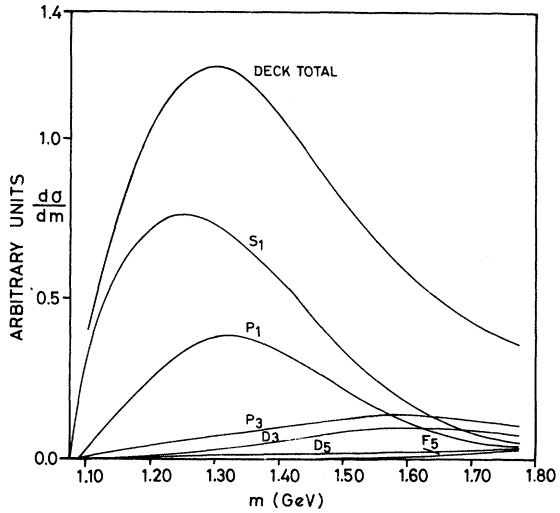

FIG. 8. Deck-model [Fig. 3(b)] predictions for $\int(d^2\sigma/dmdt)dt$, where the integral runs over $0 < t' < 0.1$ GeV^2, for partial waves as indicated, and for the sum over all partial waves; calculated from Eqs. (3.1) and (3.2) with form factor $F(\Delta^2) = \exp[-2(\Delta^2+\mu^2)^2]$.

C. Inclusion of resonances

The production amplitude and phase of a Breit-Wigner resonance of mass m_k and width $\Gamma(m)$ are taken as[12]

$$R_k = \left[\frac{m m_k \Gamma(m)\Gamma(m_k)}{(m_k^2 - m^2)^2 + m_k^2\Gamma^2(m)}\right]^{1/2}, \tag{3.5}$$

and

$$\phi_k = \tan^{-1}\left(\frac{m_k\Gamma(m)}{m_k^2 - m^2}\right), \tag{3.6}$$

and the width $\Gamma(m_k)$ is given by Eqs. (A1) and (A8) of Ref. 12. [Note that we refer to $d\sigma/dm$ and not $d\sigma/dm^2$ as in Ref. 12. We have also chosen $R_k(m = m_k) = 1$.]

Lastly we include an unknown additive phase angle $\phi_{o,k}$, to be determined for each resonance in fitting the data. All known $N^*_{1/2}$ resonances (five of them, see Table I) of mass < 1.7 GeV were included; masses and widths were given their listed values[21] in the case of the $D_3(1520)$, $D_5(1670)$, and $F_5(1688)$, but left as unknowns to be fitted in the case of the $S_1(1535)$ and $P_1(1470)$. The full amplitude for any partial wave k was then taken to be

$$A_k = x_1 f(x_2) D_k + x_k R_k e^{i(\phi_k + \phi_{o,k})}, \tag{3.7}$$

where the amounts of the resonances are adjusted by the unknowns x_k, and of the Deck contribution by the parameter x_1. The factor $f(x_2)$ is a small

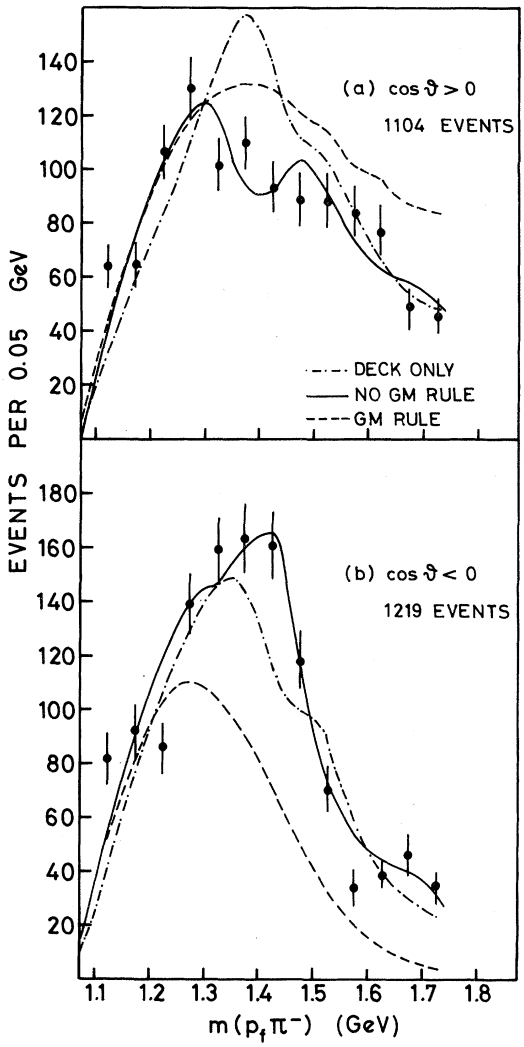

FIG. 9. Mass distributions for the data of Fig. 8 for the Gottfried-Jackson frame decay angle cuts (a) $\cos\theta > 0$, (b) $\cos\theta < 0$. The curves are as described for Fig. 8.

correction to avoid the possibility of double counting (in the duality sense) in A_k, by reducing the Deck contribution at high $N\pi$ mass and thereby allowing for any π exchange "contained" in R_k. In practice a suitable form, giving a smooth fall-off with increasing mass, was found to be

$$f(x_2) = 1.0, \quad m < 1.3 \text{ GeV},$$

$$f(x_2) = \exp(-x_2(m-1.3)^2), \quad m \geq 1.3 \text{ GeV},$$

where x_2 is an adjustable parameter. To fit the data it was found that $x_2 = (1.27 \pm 0.53)$ GeV^{-2}, thereby reducing the total Deck contribution by ~5–10% in all.

IV. FITTING TO THE DATA

The data of Fig. 4 were fitted by minimizing χ^2 defined by

$$\chi^2 = \sum_{\substack{\text{mass}\\ \text{bins}}} \sum_{ij} (\sigma_i^{\text{meas}} - \sigma_i^{\text{fit}})^\dagger G_{ij} (\sigma_j^{\text{meas}} - \sigma_j^{\text{fit}}), \quad (4.1)$$

where σ_i^{meas} is the vector of measured quantities N_i, $\langle N_i Y_{J0}\rangle (J = 1, \ldots 5)$ in any mass bin, and σ_i is the vector calculated from Eqs. (3.7) and (2.3)–(2.8); G_{ij} is the inverse of the error matrix $\langle \delta\sigma_i^{\text{meas}} \delta\sigma_j^{\text{meas}}\rangle$. At each beam momentum the 13 mass bins meant a total of 78 points to be fitted by adjusting the 16 parameters described in the previous section. Unique fits were obtained with χ^2/n_D of 1.6, and 2.0 at 20 GeV/c and 13 GeV/c, respectively, and are shown as the solid curves in Fig. 4, where the trend of the data is seen to be generally well explained. The slightly worse χ^2 for 13 GeV/c comes from the large experimental values of $\langle Y_{20}\rangle$ just above threshold. One cannot explain this, except as a statistical fluctuation, without postulating the existence of a new resonance just above threshold. We are able to discount any residual effect of the Δ.

Table I shows the contributions to the cross section at each momentum of the Deck diagram and each resonance separately; values of masses, widths, and phases were in agreement at the two momenta within the ranges shown. The S_1 and P_1 resonance masses are seen to be significantly lower than the listed values but this fact should probably not be taken too seriously in view of the dual relationship of Figs. 3(b) and 3(c). The Deck contribution was fairly independent of beam momentum, but the amounts of S_1 and P_1 resonances varied considerably. The momentum dependence of the solutions is shown more vividly in the plots of imaginary versus real parts of the whole amplitude (3.7) shown in Fig. 10. Further fitting was done with events in the smaller t' range (data set C) and gave similar answers; the results are listed in Table I and shown as the solid curves in Figs. 7 and 9. The phase ϕ_0 requires theoretical explanation; naively a Pomeron signature factor in the amplitude of Fig. 3(b) would lead one to expect $\phi_0 = \frac{1}{2}\pi$ for all resonances. A desirable improvement of the model would be to use a Reggeized pion in the Deck amplitude with its signature factor $\exp[-i\frac{1}{2}\pi\alpha_\pi(\Delta^2)]$. However, it seems very unlikely that this could alter significantly the sizes of the different resonant contributions nor account for the very large difference between the values of ϕ_0 for the different resonances (particularly the S_1 and P_1 resonances), since the major contribution to the Deck amplitude comes from $\Delta^2 \lesssim 0.2$, when the Regge phase is only $\lesssim 20^\circ$.

TABLE I. Results of fits to diffractive events $np \to (p_f \pi^-) p_s$ for the data sets indicated (see Section II B) using the amplitude of Eq. (3.7). The experimental cross sections at 13 GeV/c and 20 GeV/c were normalized to an $np \to pp\pi^-$ cross section at these momenta of 0.92 mb and 0.73 mb, respectively.[14] The solid curves in Figs. 4, 7, and 9 correspond to these fits.

Amplitude	Fitted mass range (MeV)	Fitted width (MeV)	Phase ϕ_0 (degrees)	Cross section (μb) 13 GeV/c $t' < 0.2$ (Set A)	20 GeV/c $t' < 0.2$ (Set B)	16.6 GeV/c $t' < 0.1$ (Set C)
Deck	•••	•••	•••	247±17	261±13	280±14
$S_1(1535)$	1400–1420	145±30	0±16	69±21	181±22	211±30
$P_1(1470)$	1400–1425	273±90	146±23	334±30	82±22	98±7
$D_3(1520)$	1520	125	125±75	13±7	13±4	7±2
$D_5(1670)$	1670	140	31±41	19±4	12±5	7±2
$F_5(1688)$	1688	140	0±20	6±6	11±3	5±4
Total fitted cross section (including interferences)				455	388	361
Experimental cross section				459±12	391±9	362±8
Number of events				1290	1807	2323
χ^2 of fit				127	102	126

Having established that our model amplitude gives a good phenomenological fit to the data without any parity-change rule, we next tested the GM rule in the following ways: (i) by allowing only the P_1, D_3, and F_5 resonances to contribute together with the Deck amplitude, and (ii) in an extreme form of the rule by suppressing all but the P_1,

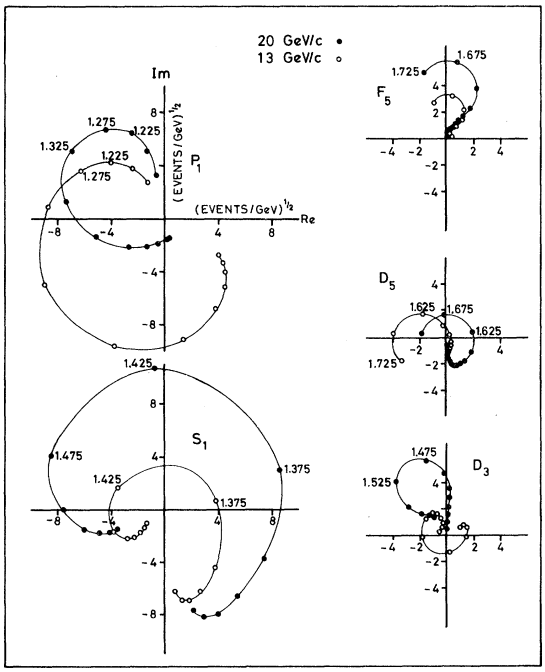

FIG. 10. Plots of imaginary versus real of the whole amplitude [Eq. (3.7)] obtained as best fit with the model described in Sec. IV, without the Gribov-Morrison rule, corresponding to the data and solid curves of Fig. 4.

D_3, and F_5 waves in the Deck amplitude as well (which as we see in Fig. 7, contains a large S_1 contribution). In (i), a poorer fit ($\chi^2/n_D \sim 3$) was obtained than previously, shown by the dashed curves in Fig. 4; it fails to reproduce the dip in $\langle Y_{10} \rangle$ near 1.4 GeV, particularly noticeable at 20 GeV/c. It is perhaps worth remarking that this feature was satisfactorily accounted for in the previous (i.e., non-GM rule) fit as due mostly to interference between the S_1 resonance and the P_1 and P_3 Deck partial waves. The poor result of a similar fit to the data set C is shown as the dashed curves in Figs. 8 and 9. In case (ii), only poor fits to the data could be obtained (not shown), with $\chi^2/n_D \sim 4$–5. Other hypothesis were tried, e.g., allowing only P_1, D_3, and F_5 resonances (i.e., no Deck contribution) but with masses and widths free; no acceptable fits were obtained.

Concerning the cross sections for resonance production given in Table I, we may compare these with the counter measurements of the process $pp \to N^* p$ at 6–30 GeV/c of Edelstein *et al.*[22] Allowing for t dependence, $N^* \to N\pi$ branching ratio, and isospin, we estimate cross sections for the equivalent diffractive process $pp \to (n\pi^+)p$ to be

$$N^*(1410) + N^*(1500) \approx 170\ \mu\text{b},$$

$$N^*(1690) \approx 80\ \mu\text{b},$$

whereas Table I gives (on average)

$$S_1(1535) + P_1(1470) + D_3(1520) \approx 346\ \mu\text{b},$$

$$D_5(1670) + F_5(1688) \approx 24\ \mu\text{b}.$$

Considering the very different techniques for handling background and identifying resonances,

the difference between these figures is hardly surprising.

Finally, we may compare the Table I cross-section values with those from πN phase-shift analyses. Using the listed[21] values of masses and widths, we calculate the values of $4\pi\lambda^2(J+\frac{1}{2})(\Gamma_{el}/\Gamma)^2$ in mb for each of the resonances in the order of Table I to be 2.8, 10.0, 14.2, 7.5, and 16.0. Our analysis points to a much enhanced role for the $J=\frac{1}{2}$ resonances in diffractive production as compared to elastic scattering.

V. SUMMARY AND CONCLUSION

A Deck-plus-resonance model amplitude has been described and applied to diffractive events $np \to (p_f\pi^-)p_s$ at 13 GeV/c and 20 GeV/c. The influence of an apparently small degree of TCHC violation has been discussed. When $p_f\pi^-$ spin states up to $j=\frac{5}{2}$ are used, a satisfactory fit to the experimental data ($\chi^2/n_D \sim 1.6$–2) could be obtained provided those states which the proposed Gribov-Morrison rule would otherwise exclude, particularly the $j=\frac{1}{2}^-$ state (S_1 partial wave), are included. The $\langle Y_{10}\rangle$ moment plays an important role in showing that this partial wave is required.

ACKNOWLEDGMENTS

We are grateful to B. R. Webber for helpful discussions. R. R. acknowledges the financial support of Trinity College, Cambridge.

*Work supported by the Science Research Council, U.K.

[1]See for example, D. R. O. Morrison, in *Proceedings of the Fifth Hawaii Topical Conference in Particle Physics, 1973,* edited by P. N. Dobson *et al.* (University Press of Hawaii, Honolulu, 1974), p. 189.
[2]D. R. O. Morrison, Phys. Rev. 165, 1699 (1968).
[3]V. N. Gribov, Yad Fiz. [Sov. J. Nucl. Phys.] 5, 197 (1967).
[4]G. Ascoli *et al.*, Phys. Rev. D 7, 669 (1973); Yu. M. Antipov *et al.*, Nucl. Phys. B63, 153 (1973).
[5]M. Deutschman *et al.*, Phys. Lett. 49B, 388 (1974).
[6]V. E. Kruse *et al.*, Phys. Rev. Lett. 32, 1328 (1974).
[7]D. Lissauer *et al.*, Phys. Rev. D 6, 1852 (1972); J. W. Cooper *et al.*, Nucl. Phys. B79, 259 (1974).
[8]W. Ochs *et al.*, Nucl. Phys. B86, 253 (1975).
[9]D. R. O. Morrison, in *Proceedings of the Fifteenth International Conference on High Energy Physics, Kiev, 1970,* edited by V. Shelest (Naukova Dumka, Kiev, U. S. S. R., 1972).
[10]J. G. Rushbrooke, in *Proceedings of the Third International Colloquium on Multiparticle Reactions, Zakopane, Poland, 1972,* edited by O. Czyzewski and L. Michejda (Nuclear Energy Information Center of the Polish Government, Warsaw, 1972), p. 442.
[11]R. F. Peierls and T. L. Trueman, Phys. Rev. 134, B1365 (1964).
[12]J. D. Jackson, Nuovo Cimento 34, 1644 (1964).
[13]A. D. Martin and T. D. Spearman, *Elementary Particle Theory* (North-Holland, Amsterdam, 1970); also B. R. Webber, private communication.
[14]R. Raja, Ph.D. thesis, University of Cambridge, 1975 (unpublished); D. R. Ward, Nucl. Phys. B92, 101 (1975).
[15]E. Dahl-Jensen *et al.*, Nucl. Phys. B87, 426 (1975).
[16]H. Grässler *et al.*, Nucl. Phys. B95, 1 (1975).
[17]E. L. Berger, Argonne Report No. ANL HEP PR 75 32, 1975, (unpublished).
[18]E. L. Berger and A. C. Irving, Phys. Rev. D 12, 3444 (1975).
[19]L. Resnick, Phys. Rev. 150, 1292 (1966).
[20]J. G. Rushbrooke, Phys. Rev. 177, 2357 (1969).
[21]Particle Data Group, Phys. Lett. 50B, 1 (1974).
[22]R. M. Edelstein *et al.*, Phys. Rev. D 5, 1073 (1972).